

## Modulation instability in nonlinear negative-index material

Shuangchun Wen,\* Youwen Wang, Wenhua Su, Yuanjiang Xiang, Xiquan Fu, and Dianyuan Fan

Laboratory of Information Optoelectronics and School of Computer and Communication, Hunan University, Changsha 410082, China

(Received 20 December 2005; published 24 March 2006)

We investigate modulation instability (MI) in negative-index material (NIM) with a Kerr nonlinear polarization based on a derived (3+1)-dimensional nonlinear Schrödinger equation for ultrashort pulse propagation. By a standard linear stability analysis, we obtain the expression for instability gain, which unifies the temporal, spatial, and spatiotemporal MI. It is shown that negative refraction not only brings some new features to MI, but also makes MI possible in ordinary material in which it is otherwise impossible. For example, spatial MI can occur in the defocusing regime, while it only occurs in the focusing regime in ordinary material. Spatiotemporal MI can appear in NIM in the case of anomalous dispersion and defocusing nonlinearity, while it cannot appear in ordinary material in the same case. We believe that the difference between the MI in NIM and in ordinary material is due to the fact that negative refraction reverses the sign of the diffraction term, with the signs of dispersion and nonlinearity unchanged. The most notable property of MI in NIM is that it can be manipulated by engineering the self-steepening effect by choosing the size of split-ring resonator circuit elements. To sum up the MI in ordinary material and in NIM, MI may occur for all the combinations of dispersion and nonlinearity.

DOI: [10.1103/PhysRevE.73.036617](https://doi.org/10.1103/PhysRevE.73.036617)

PACS number(s): 41.20.Jb, 42.65.Sf, 42.25.Bs, 42.65.Re

### I. INTRODUCTION

Over three decades ago, Veselago [1] demonstrated theoretically that a material in which both the dielectric permittivity  $\epsilon$  and magnetic permeability  $\mu$  are negative would also allow the propagation of electromagnetic waves. The refractive index of such a material is negative, and thus it is called negative index material (NIM). Although there are no known naturally occurring NIMs, artificially designed materials (metamaterials) can act as NIMs. Since the experimental confirmation of negative refraction in the metal-dielectric metamaterials at microwave wavelengths [2,3], there has been intense interest in NIMs. In the meanwhile, negative refraction in the near-IR range have been experimentally demonstrated in GaAs-based photonic crystals [4] and in a Si-polyimide photonic crystals [5], respectively. NIMs at optical wavelengths will also be obtainable before long [6]. Additionally, nonlinear NIMs can also be created [7–9]. For example, Zharov *et al.* [7] demonstrated that a two-dimensional periodic structure created by arrays of wires and split-ring resonators embedded into a nonlinear dielectric takes on a Kerr-type dielectric permittivity.

Recently, there has been a great deal of research on the propagation of electromagnetic radiation in NIMs [10–16]. Most research, however, is on the propagation of plane waves in the linear regime. Some authors have demonstrated the basic dynamics of short pulses undergoing negative refraction in the linear propagation regime [13–16]. A natural extension is the nonlinear propagation of ultrashort pulse in NIM [11,17–19]. The study of the nonlinear propagation of ultrashort pulses in NIMs could lead to completely new electronic and optical devices. Very recently, several papers have been published on the nonlinear propagation of ultrashort

pulses in NIMs. In Ref. [17], Lazarides and Tsironis derived a system of coupled nonlinear Schrödinger equations for the envelopes of the propagating electric and magnetic fields in an isotropic, homogeneous, quasi-one-dimensional NIM. Based on the coupled nonlinear Schrödinger equations, Kourakis and Shukla have investigated the nonlinear stability of electromagnetic waves in NIM, and obtained the modulational stability profile of the coupled plane-wave solutions [18]. Scalora *et al.* [19] investigated the propagation of pulses at least a few tens of optical cycles in duration in NIM with a nonlinear polarization, and obtained a new generalized nonlinear Schrödinger equation for the envelope of the propagating electric field in which the linear and nonlinear coefficients can be tailored through the linear properties of the medium to attain any combination of signs unachievable in ordinary matter, showing a significant potential to realize a wide class of solitary waves.

In this paper, we investigate modulation instability (MI) in NIM with a Kerr nonlinearity. MI of continuous wave (cw) or quasi-cw is an issue closely related to the existence of both bright and dark solitons. It is probably the most remarkable nonlinear phenomena that may occur in nature. In nonlinear optics, MI can be classified as temporal [20,21], spatial (or transverse) [22,23], and spatiotemporal [24,25]. The temporal MI occurs due to the interplay between nonlinearity and group velocity dispersion (GVD) and manifests itself as the breakup of cw or quasi-cw into a train of ultrashort pulses. The spatial MI occurs as a result of the interaction between nonlinearity and diffraction and manifests itself as the breakup of an otherwise homogeneous beam into numerous small filaments. It is also known as small-scale self-focusing in which diffraction plays the same role as anomalous GVD in the case of temporal MI. Unlike independently occurring temporal MI and spatial MI, the spatiotemporal MI occurs due to the simultaneous presence of temporal and spatial MI in a nonlinear medium. MI in NIMs remains essentially unexplored. To disclose the properties of

\*Electronic address: scwen@hnu.cn

MI in NIMs, we first derive a propagation model for (3+1)-dimensional ultrashort pulses in NIM characterized by a Drude model of both  $\varepsilon$  and  $\mu$ . Then we present a linear stability analysis to obtain the expression for instability gain. Based on the obtained expression, we further clarify three kinds of MI, i.e., temporal, spatial, and spatiotemporal MI in NIM, and compare them to those in ordinary dispersive media and explain the differences. We find some new features of MI in NIMs, demonstrating that NIMs provide a new choice for soliton generation.

## II. (3+1)-DIMENSIONAL MODEL FOR PULSE PROPAGATION IN NIMs

We first present a derivation of a (3+1)-dimensional evolution equation for an envelope description of pulse propagation in the NIM with a nonlinear polarization. Our approach differs from that of Ref. [19] in that we eliminate the magnetic field at the very start. This makes it possible for us to derive the propagation equation by following the same procedure as in ordinary materials. It is easy to show that, from Maxwell equations, we can obtain the following three-dimensional wave equation:

$$\left(\frac{\partial^2}{\partial z^2} + \nabla_{\perp}^2\right)E(\vec{r}, t) = \mu\varepsilon \frac{\partial^2 E(\vec{r}, t)}{\partial t^2} + \mu \frac{\partial^2 P_{nl}(\vec{r}, t)}{\partial t^2}, \quad (1)$$

where  $\nabla_{\perp}^2$  is the transverse Laplace operator. The electric field  $E$  propagates along the  $z$  direction. Both  $E$  and the nonlinear polarization  $P_{nl}$  are assumed to be polarized parallel to the  $x$  axis.

It is known that  $\varepsilon$  and  $\mu$  in a NIM have to be dispersive, otherwise the energy density could be negative [1]. Their frequency dispersion can be described by a lossy Drude model [26],

$$\varepsilon(\omega) = \varepsilon_0 \left[ 1 - \frac{\omega_{pe}^2}{\omega(\omega + i\gamma_e)} \right], \quad \mu(\omega) = \mu_0 \left[ 1 - \frac{\omega_{pm}^2}{\omega(\omega + i\gamma_m)} \right], \quad (2)$$

where  $\omega$  is frequency,  $\omega_{pe}$  and  $\omega_{pm}$  are the respective electric and magnetic plasma frequencies,  $\gamma_e$  and  $\gamma_m$  are the respective electric and magnetic loss terms, which are very small and are neglected in the following analysis for simplicity, and  $\varepsilon_0$  and  $\mu_0$  are the respective vacuum permittivity and magnetic permeability. The negative refraction behavior is restricted within a certain range of frequency values. We can transform Eq. (1) into frequency space in order to expand  $\varepsilon(\omega)$  and  $\mu(\omega)$  in powers of  $\omega$ , thus enabling us to treat the material parameters as a power series which we can truncate to an appropriate order. However, for simplicity it is better to expand  $\omega\varepsilon(\omega)$  and  $\omega\mu(\omega)$  about a suitable  $\omega_0$  instead,

$$\omega\varepsilon(\omega) = \sum_{n=0}^{\infty} \left\{ \frac{\partial^n[\omega\varepsilon(\omega)]}{\partial \omega^n} \Big|_{\omega=\omega_0} \frac{(\omega - \omega_0)^n}{n!} \right\}, \quad (3)$$

$$\omega\mu(\omega) = \sum_{n=0}^{\infty} \left\{ \frac{\partial^n[\omega\mu(\omega)]}{\partial \omega^n} \Big|_{\omega=\omega_0} \frac{(\omega - \omega_0)^n}{n!} \right\}. \quad (4)$$

We can now write the frequency space version of Eq. (1) as

$$\begin{aligned} & \left(\frac{\partial^2}{\partial z^2} + \nabla_{\perp}^2\right)\tilde{E}(\vec{r}, \omega) \\ &= - \sum_{m=0}^{\infty} \left\{ \frac{\partial^m(\omega\varepsilon)}{\partial \omega^m} \Big|_{\omega=\omega_0} \frac{(\omega - \omega_0)^m}{m!} \right\} \\ & \times \sum_{n=0}^{\infty} \left\{ \frac{\partial^n(\omega\mu)}{\partial \omega^n} \Big|_{\omega=\omega_0} \frac{(\omega - \omega_0)^n}{n!} \right\} \tilde{E}(\vec{r}, \omega) - \omega \\ & \times \sum_{n=0}^{\infty} \left\{ \frac{\partial^n(\omega\mu)}{\partial \omega^n} \Big|_{\omega=\omega_0} \frac{(\omega - \omega_0)^n}{n!} \right\} \tilde{P}_{nl}(\vec{r}, \omega), \quad (5) \end{aligned}$$

where  $\tilde{E}$  and  $\tilde{P}_{nl}$  are the Fourier transforms of  $E$  and  $P_{nl}$ , respectively. We introduce an envelope and carrier form for the field in the usual way, using  $\vec{r} = (\vec{r}_{\perp}, z)$ ,  $\vec{r}_{\perp} = (x, y)$ , so that,  $E(\vec{r}_{\perp}, z, t) = A(\vec{r}_{\perp}, z, t) \exp(ik_0 z - i\omega_0 t) + c.c.$ , where  $k_0 = n(\omega_0)\omega_0/c$ , and  $n(\omega_0)$  is the refractive index of the material at  $\omega_0$ . In addition, we assume that  $P_{nl}(\vec{r}, t) = \varepsilon_0 \chi^{(3)} |E(\vec{r}_{\perp}, z, t)|^2 E(\vec{r}_{\perp}, z, t)$ , where  $\chi^{(3)}$  is the third-order susceptibility, which characterizes a Kerr nonlinearity. With these envelope-carrier substitutions, and taking the inverse Fourier transform of the obtained equation, we have

$$\begin{aligned} & \left(\frac{\partial^2}{\partial z^2} + 2ik_0 \frac{\partial}{\partial z} - k_0^2 + \nabla_{\perp}^2\right)A \\ &= - \sum_{m=0}^{\infty} \left\{ D_m \frac{\partial^m A}{\partial t^m} \right\} - \varepsilon_0 \chi^{(3)} \omega_0 F_0 |A|^2 A - \varepsilon_0 \chi^{(3)} \\ & \times \sum_{m=1}^{\infty} \left[ (iF_{m-1} + \omega_0 F_m) \frac{\partial^m}{\partial t^m} (|A|^2 A) \right], \quad (6) \end{aligned}$$

where

$$D_m = \sum_{l=0}^m \frac{i^m}{l!(m-l)!} \frac{\partial^l(\omega\varepsilon)}{\partial \omega^l} \Big|_{\omega=\omega_0} \frac{\partial^{m-l}(\omega\mu)}{\partial \omega^{m-l}} \Big|_{\omega=\omega_0} \quad (7)$$

and

$$F_m = \frac{i^m}{m!} \frac{\partial^m[\omega\mu(\omega)]}{\partial \omega^m} \Big|_{\omega=\omega_0}. \quad (8)$$

Introducing comoving variables,  $\tau = t - z/V$ ,  $\xi = z$ , where  $V = 2k_0/(\omega_0\varepsilon\gamma + \omega_0\mu\alpha)$ ,  $\alpha = \partial[\omega\varepsilon(\omega)]/\partial\omega|_{\omega=\omega_0}$ ,  $\gamma = \partial[\omega\mu(\omega)]/\partial\omega|_{\omega=\omega_0}$ , Eq. (6) is transformed to

$$\begin{aligned} 2ik_0 \frac{\partial A}{\partial \xi} &= - \nabla_{\perp}^2 A - \frac{1}{V^2} \frac{\partial^2 A}{\partial \tau^2} - \sum_{m=2}^{\infty} \left\{ D_m \frac{\partial^m A}{\partial \tau^m} \right\} - \frac{\partial^2 A}{\partial \xi^2} + \frac{2}{V} \frac{\partial^2 A}{\partial \tau \partial \xi} \\ & - \omega_0 \varepsilon_0 \chi^{(3)} F_0 |A|^2 A - \varepsilon_0 \chi^{(3)} \sum_{m=1}^{\infty} \left[ (iF_{m-1} + \omega_0 F_m) \right. \\ & \left. \times \frac{\partial^m}{\partial \tau^m} (|A|^2 A) \right]. \quad (9) \end{aligned}$$

In deriving Eq. (9), we have not made further approximations. It is suitable for few-cycle pulse propagation in NIM, and is thus more general than Eq. (12) in Ref. [19]. In fact, by using the same approximations as Ref. [19], one can eas-

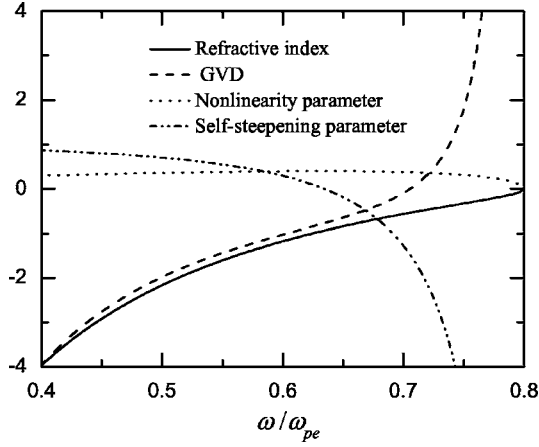


FIG. 1. Refractive index  $n$ , GVD  $\beta_2$ , nonlinearity parameter  $C_{nl}$  (here we assume  $\chi^{(3)} > 0$ ), and self-steepening parameter  $C_s$  vs  $\omega/\omega_{pe}$  for  $\omega_{pm}/\omega_{pe}=0.8$ .  $C_{nl}$  is calculated in units of  $\chi^{(3)}/(2c)$ ,  $\beta_2$  in units of  $1/(2\pi c\omega_{pe})$ , and  $C_s$  in units of  $1/\omega_0$ .

ily show that Eq. (12) in Ref. [19] is recovered by our Eq. (9).

To explicitly demonstrate the fundamental aspect of MI in NIM, we keep the dispersion coefficients to second order and neglect all higher-order derivatives ( $m \geq 2$ ) with respect to the nonlinearity. Equation (9) is thus reduced to

$$\frac{\partial A}{\partial \xi} = \frac{i}{2k_0} \nabla_{\perp}^2 A - \frac{i\beta_2}{2} \frac{\partial^2 A}{\partial \tau^2} + iC_{nl} \left( 1 + iC_s \frac{\partial}{\partial \tau} \right) (|A|^2 A), \quad (10)$$

where  $\beta_2$ ,  $C_{nl}$ , and  $C_s$  are the GVD, nonlinear, and self-steepening coefficients, respectively. They are defined as

$$\beta_2 = (\alpha\gamma + \omega_0\mu\alpha'/2 + \omega_0\varepsilon\gamma'/2 - 1/V^2)/k_0, \quad (11)$$

$$C_{nl} = \omega_0\mu_r\chi^{(3)}/(2cn), \quad (12)$$

$$C_s = [1 + \gamma/\mu - \omega_0/(k_0V)]/\omega_0, \quad (13)$$

where  $\alpha' = \partial^2[\omega\varepsilon(\omega)]/\partial\omega^2|_{\omega=\omega_0}$ ,  $\gamma' = \partial^2[\omega\mu(\omega)]/\partial\omega^2|_{\omega=\omega_0}$ , and  $c$  is light velocity in vacuum.

Figure 1 shows the variation of  $n$ ,  $\beta_2$ ,  $C_{nl}$ , and  $C_s$  with  $\omega/\omega_{pe}$  for  $\omega_{pm}/\omega_{pe}=0.8$  and  $\gamma_e=\gamma_m=0$ . It shows that the zero GVD point is located at  $\omega/\omega_{pe} \approx 0.7$  in the negative refraction region. By choosing the size of split-ring resonator circuit elements, the zero GVD point can be shifted back and forth [3,16]. Compared to ordinary material, the most noticeable characteristics of the parameters of the nonlinear Schrödinger equation (10) is the anomaly of self-steepening parameter: First, the self-steepening parameter can be negative and zero, with the zero point located at  $\omega/\omega_{pe} \approx 0.634$  for the present case. Second, in the positive self-steepening region ( $\omega/\omega_{pe} < 0.634$ ), the value of the normalized self-steepening parameter is about 1, approximating the value in ordinary material, while in the negative self-steepening region ( $\omega/\omega_{pe} > 0.634$ ), it can be far larger than 1. Like the GVD parameter, the self-steepening parameter can also be engineered by choosing the size of split-ring resonator circuit

elements. The anomalous characteristics of the linear and nonlinear parameters mean that there should be anomalous phenomena of MI and soliton in NIM. Apparently, a reexamination of the two phenomena is necessary.

### III. ANALYSIS OF MODULATION INSTABILITY IN NIM

Although Kourakis and Shukla [18] have investigated the nonlinear stability of electromagnetic waves in NIM, they only considered the case of temporal MI in NIM based on a system of coupled nonlinear Schrödinger equations for both electric and magnetic pulses propagation. The system of coupled nonlinear Schrödinger equations does not include the diffraction and the anomalous self-steepening effects, and thus the characteristics of two other two kinds of MI, namely spatial and spatiotemporal MI, and the influence of the anomalous self-steepening effect on MI, are not disclosed. Here, we first derive a general expression for MI gain in NIM by a standard linear stability analysis based on Eq. (10), and then clarify three kinds of MI.

#### A. Derivation of the expression for MI gain in NIM

Apparently, Eq. (10) has the continuous wave (cw) solution,  $A(x, y, \xi, \tau) = A_0 \exp(ib\xi)$ , where  $A_0$  is the amplitude of the cw solution,  $b = C_{nl}A_0^2$ . We assume that the cw solution is slightly perturbed such that

$$A(x, y, \xi, \tau) = A_0[1 + a(x, y, \xi, \tau)] \exp(ib\xi), \quad (14)$$

where the perturbation  $|a| \ll 1$ . Substituting Eq. (14) into Eq. (10) and linearizing in  $a$ , we obtain the evolution equation for  $a$ ,

$$\frac{\partial a}{\partial \xi} = \frac{i}{2k_0} \nabla_{\perp}^2 a - \frac{i\beta_2}{2} \frac{\partial^2 a}{\partial \tau^2} + ib(a + a^*) - 2C_s b \frac{\partial a}{\partial \tau} - C_s b \frac{\partial a^*}{\partial \tau}. \quad (15)$$

Decomposing the perturbation into real and imaginary parts,  $a = u + iv$ , we obtain two coupled equations,

$$\frac{\partial u}{\partial \xi} = -\frac{1}{2k_0} \nabla_{\perp}^2 v + \frac{\beta_2}{2} \frac{\partial^2 v}{\partial \tau^2} - 3C_s b \frac{\partial u}{\partial \tau},$$

$$\frac{\partial v}{\partial \xi} = \frac{1}{2k_0} \nabla_{\perp}^2 u - \frac{\beta_2}{2} \frac{\partial^2 u}{\partial \tau^2} + 2bu - C_s b \frac{\partial v}{\partial \tau}. \quad (16)$$

By introducing the Fourier transforms

$$\begin{aligned} \tilde{u}(q_x, q_y, \omega, \xi) &= \int \int \int_{\infty} u(x, y, \tau, \xi) \\ &\quad \times \exp[i(q_x x + q_y y + \omega \tau)] dx dy d\tau, \\ \tilde{v}(q_x, q_y, \omega, \xi) &= \int \int \int_{\infty} v(x, y, \tau, \xi) \\ &\quad \times \exp[i(q_x x + q_y y + \omega \tau)] dx dy d\tau, \end{aligned} \quad (17)$$

where  $q = (\sqrt{q_x^2 + q_y^2})$  and  $\omega$  are the transverse wave number and frequency for the perturbation, respectively, the linear-

ized system (16) is converted to a set of ordinary differential equations in frequency space,

$$\frac{\partial}{\partial \xi} \begin{pmatrix} \tilde{u} \\ \tilde{v} \end{pmatrix} = \begin{pmatrix} m_{11} & m_{12} \\ m_{21} & m_{22} \end{pmatrix} \begin{pmatrix} \tilde{u} \\ \tilde{v} \end{pmatrix}, \quad (18)$$

where  $m_{11} = -i3C_s b \varpi$ ,  $m_{12} = q^2/(2k_0) - \beta_2 \varpi^2/2$ ,  $m_{21} = -q^2/(2k_0) + \beta_2 \varpi^2/2$ , and  $m_{22} = -iC_s b \varpi$ . The positive real part of the eigenvalue of the coefficient matrix corresponds to the instability gain  $G$ ,

$$G = \sqrt{\left(\frac{q^2}{2k_0} - \frac{\beta_2 \varpi^2}{2}\right) \left(2b - \frac{q^2}{2k_0} + \frac{\beta_2 \varpi^2}{2}\right) - C_s^2 b^2 \varpi^2}. \quad (19)$$

For convenience, we introduce a characteristic frequency,  $\varpi_c = 2\sqrt{|b/\beta_2|}$ , and make the substitutions,  $\kappa = q/(2\sqrt{|k_0 b|})$ ,  $\sigma = \varpi/\varpi_c$ ,  $g = G/|b|$ ,  $s = C_s \varpi_c$ , to transform Eq. (19) into the following normalized form:

$$g = \sqrt{4[\text{sgn}(n)\kappa^2 - \text{sgn}(\beta_2)\sigma^2][\text{sgn}(\chi^{(3)}) - \text{sgn}(n)\kappa^2 + \text{sgn}(\beta_2)\sigma^2] - s^2\sigma^2}. \quad (20)$$

In the case when instability occurs, it is interesting to find a particular perturbation mode that provides for a maximum instability gain. Such a mode, which is usually called the fastest growing mode, can be found from Eq. (20) by setting  $\partial g/\partial \kappa = 0$ ,  $\partial g/\partial \sigma = 0$ , and its spatial and temporal frequencies are such that

$$\text{sgn}(n)\kappa_{\max}^2 - \text{sgn}(\beta_2)\sigma_{\max}^2 = \text{sgn}(\chi^{(3)})/2, \quad (21)$$

and the corresponding maximum gain is

$$g_{\max} = \sqrt{1 - s^2\sigma^2}. \quad (22)$$

The general expressions (20)–(22) form the basis of our further analysis. As is well known and demonstrated in Fig. 1, negative refraction behavior is restricted within a certain range of frequency values. Thus, Eqs. (20)–(22) formally apply to both ordinary materials and NIMs. In addition, Eq. (20) unifies all three kinds of MI in NIM: (i) by setting  $\kappa = 0$ , we obtain the gain expression for temporal MI; (ii) by setting  $\sigma = 0$ , we obtain the gain expression for spatial MI, also called small-scale self-focusing. Further, it is obvious that whether MI occurs depends on not only the combination of the signs of  $n$ ,  $\beta_2$ , and  $\chi^{(3)}$ , as in ordinary material, but also on the value of self-steepening parameter  $s$ . As Fig. 1 shows, the self-steepening parameter can be large enough to make the modulation gain be imaginary, meaning MI cannot occur. Equations (21) and (22) show that for occurring MI, the self-steepening effect reduces the maximum gain, yet does not influence the fastest growing frequencies.

## B. Features of the three kinds of MI in NIM

Modulation instability in ordinary materials with  $\text{sgn}(n) = 1$  has been well understood. We thus focus our attention on the case of  $\text{sgn}(n) = -1$  for different combinations of the signs of  $\beta_2$  and  $\chi^{(3)}$  to disclose the properties of temporal, spatial, and spatiotemporal MIs in NIMs, respectively.

### 1. Temporal MI in NIM

The expression for temporal MI gain is obtained from Eq. (20) by setting  $\kappa = 0$ ,

$$g = \sqrt{-4 \text{sgn}(\beta_2)\sigma^2[\text{sgn}(\chi^{(3)}) + \text{sgn}(\beta_2)\sigma^2] - s^2\sigma^2}, \quad (23)$$

which is the same as that for MI in ordinary material [20,21]. For focusing nonlinearity, MI occurs in the anomalous dispersion regime, while for defocusing nonlinearity, MI occurs in the normal dispersion regime. This similarity can be explained as follows. For one thing, temporal MI occurs only when nonlinearity and dispersion act in opposition: when nonlinearity is positive (focusing), GVD must be anomalous; if nonlinearity is negative (defocusing), GVD must be normal. For another thing, although negative refraction alters the sign of wave number  $k_0$ , it does not alter the sign of the nonlinearity coefficient determined by the combination of signs of  $\mu$ ,  $n$ , and  $\chi^{(3)}$ , as Eq. (12) shows. For NIM,  $\mu$  and  $n$  are simultaneously negative, and thus the sign of the nonlinearity coefficient is only determined by  $\chi^{(3)}$ , as in ordinary materials. The similarity means that negative refraction of material does not influence the temporal property of the fundamental soliton propagation.

The self-steepening effects in NIM and in ordinary material are quite different. First, the self-steepening effect in NIM can be positive and negative, as is shown in Ref. [19] and in Fig. 1. Secondly, the self-steepening coefficient  $C_s$  may be very large in NIM, and even far larger than in ordinary material. The first difference does not alter the role of the self-steepening effect in MI in NIM, as is shown in Eq. (23), which shows that MI in NIM is independent of the sign of the self-steepening coefficient. The second difference, however, is most notable, which may lead to quite different results. In NIM, the self-steepening effect suppresses MI by reducing the maximum MI gain and shrinking the gain band when

$$s^2 < -4[\text{sgn}(\chi^{(3)})\text{sgn}(\beta_2) + \sigma^2], \quad (24)$$

as it does in ordinary material, and eliminates MI when

$$s^2 > -4[\text{sgn}(\chi^{(3)})\text{sgn}(\beta_2) + \sigma^2]. \quad (25)$$

Figure 2 is the plot of MI gain  $g$  versus  $\sigma$  for different values of self-steepening coefficient  $s$ . We see that the MI gain band

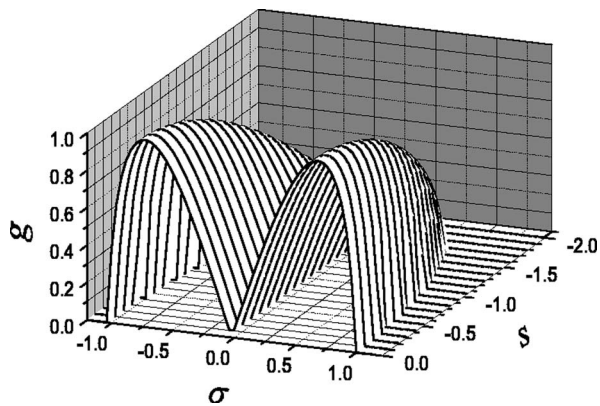


FIG. 2. Temporal MI gain spectrum in NIM with different self-steepening parameter  $s$ .

shrinks as the self-steepening coefficient increases and disappears after the self-steepening coefficient arrives at a critical value. As stated before, the self-steepening effect can be engineered, thus the MI can be manipulated. These results illustrate not only the unusual nonlinear effects that can be seen in NIMs, but also the new ways of manipulating solitons.

### 2. Spatial MI in NIM

The features of spatial MI in NIM can be obtained from the following expression for MI gain:

$$g = \sqrt{-4\kappa^2[\text{sgn}(\chi^{(3)}) + \kappa^2]}. \quad (26)$$

Apparently, spatial MI only occurs in defocusing NIM ( $\chi^{(3)} < 0$ ), contrary to that in ordinary material, in which spatial MI only occurs in the focusing regime ( $\chi^{(3)} > 0$ ). This opposition is due to the fact that negative refraction reverses the sign of the diffraction term, with the nonlinearity coefficient unchanged, as Eqs. (10) and (12) show. This result suggests that negative refraction not only reverses the conditions for the formation of spatial bright and dark solitons, and the appearance of self-focusing and self-defocusing of optical beam in nonlinear materials, but also supplies a new way of stimulating spatial MI, making MI possible in ordinary materials in which it is otherwise impossible.

### 3. Spatiotemporal MI in NIM

The results for spatiotemporal MI in NIM are summarized in density plots of gain versus temporal frequency  $\sigma$  and spatial frequency  $\kappa$  for  $s=0$  (Fig. 3). It shows that spatiotemporal MI occurs in three cases: (i) in focusing material with anomalous dispersion [Fig. 3(a)] under the condition of

$$0 < \sigma^2 - \kappa^2 < 1, \quad (27)$$

(ii) in defocusing material with normal dispersion [Fig. 3(b)] under the condition of

$$\kappa^2 + \sigma^2 < 1, \quad (28)$$

and (iii) in defocusing material with anomalous dispersion [Fig. 3(c)] under the condition of

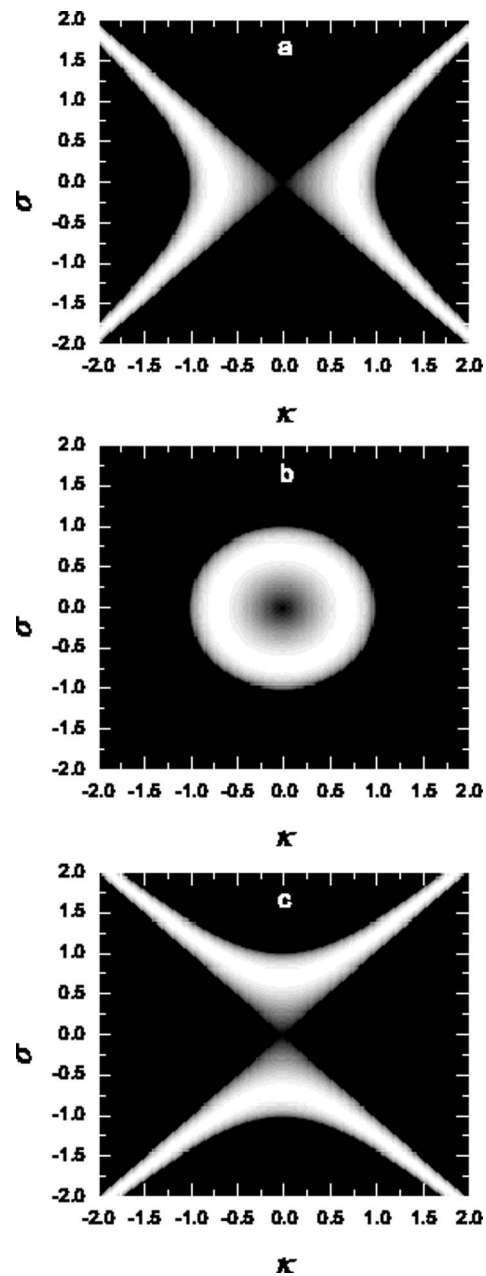


FIG. 3. Spatiotemporal MI gain in the  $(\kappa, \sigma)$  plane for the cases of (a) focusing material with anomalous dispersion, (b) defocusing material with normal dispersion, and (c) defocusing material with anomalous dispersion. The gray to white regions represent temporal and spatial frequencies to high gain on a linear scale; gain is zero in the black regions.

$$0 < \kappa^2 - \sigma^2 < 1. \quad (29)$$

Comparing the results with those in ordinary nonlinear dispersive material [24,25], we find an interesting fact that the spatiotemporal MI in NIM for a definite combination of dispersion and nonlinearity is just that in ordinary material for a combination of opposite dispersion and opposite nonlinearity. For example, the gain spectra in the three cases, corresponding to Figs. 3(a)–3(c), are, respectively, the same as those in ordinary material for the cases of (i) defocusing

nonlinearity and normal dispersion, (ii) focusing nonlinearity and anomalous dispersion, and (iii) focusing nonlinearity and normal dispersion. The physical origin of the fact is that the negative refraction reverses the phase velocity, and thus reverses the diffraction term. This leads to the diffraction and normal dispersion being equivalent when acting with nonlinearity in NIM, while in ordinary material, diffraction is equivalent with anomalous dispersion. In addition, spatiotemporal MI shows how diffraction and dispersion act together to couple space and time. It occurs due to the simultaneous presence of temporal MI and spatial MI in a nonlinear medium, unlike independently occurring temporal MI and spatial MI. Thus the three cases in which spatiotemporal MI can occur can also be obtained by combining the former two kinds of MI.

Just like temporal MI, if the role of the self-steepening effect is taken into account, the spatiotemporal MI may be suppressed and even eliminated, depending on the value of self-steepening parameter.

To sum up, supplemented by NIM, MI can occur in nonlinear optics for any combination of the signs of dispersion and nonlinearity. Spatiotemporal MI can be used to convert a cw into a train of ultrashort pulses. The anomalous MI regions in NIMs thus provide an alternative way of generating ultrashort pulses.

#### IV. CONCLUSION

We have derived a (3+1)-dimensional nonlinear Schrödinger equation for ultrashort pulse propagation in

negative-index material with Kerr nonlinearity. Based on the nonlinear Schrödinger equation, we obtain the expression for MI gain, which unifies the temporal, spatial, and spatiotemporal MI. We demonstrate that temporal MI may occur in both focusing and defocusing regimes, as in ordinary materials. Spatial MI, however, only occurs in the defocusing regime, contrary to ordinary material. Spatiotemporal MI in NIM for a definite combination of dispersion and nonlinearity is just that in ordinary material for a combination of opposite dispersion and opposite nonlinearity. We believe that the difference between the MI in NIM and in ordinary material is due to the fact that negative refraction reverses the sign of the diffraction term, with the signs of dispersion and nonlinearity unchanged. The most notable property of MI in NIM is that it can be manipulated by engineering the self-steepening effect by choosing the size of split-ring resonator circuit elements. To sum up the MI in ordinary material and in NIM, MI may occur for all the combinations of dispersion and nonlinearity. The results suggest new ways of generating solitons and ultrashort pulses, and illustrate the unusual nonlinear effects that can be seen in NIMs.

#### ACKNOWLEDGMENTS

This work is supported by the National Natural Science Foundation of China (Grants No. 10576012 and No. 60538010), the National High Technology Research and Development Program of China (Grant No. 2004AA84ts12), and the Specialized Research Fund for the Doctoral Program of Higher Education of China (Grant No. 20040532005).

- 
- [1] V. G. Veselago, *Sov. Phys. Usp.* **10**, 509 (1968).
  - [2] D. R. Smith, W. J. Padilla, D. C. Vier, S. C. Nemat-Nasser, and S. Schultz, *Phys. Rev. Lett.* **84**, 4184 (2000).
  - [3] R. A. Shelby, D. R. Smith, and S. Schultz, *Science* **292**, 77 (2001).
  - [4] A. Berrier, M. Mulot, M. Swillo, M. Qiu, L. Thylén, A. Talneau, and S. Anand, *Phys. Rev. Lett.* **93**, 073902 (2004).
  - [5] E. Schonbrun, M. Tinker, W. Park, and J.-B. Lee, *IEEE Photon. Technol. Lett.* **17**, 1196 (2005).
  - [6] J. Zhou, Th. Koschny, M. Kafesaki, E. N. Economou, J. B. Pendry, and C. M. Soukoulis, *Phys. Rev. Lett.* **95**, 223902 (2005).
  - [7] A. A. Zharov, I. V. Shadrivov, and Y. S. Kivshar, *Phys. Rev. Lett.* **91**, 037401 (2003).
  - [8] S. O'Brien, D. McPeake, S. A. Ramakrishna, and J. B. Pendry, *Phys. Rev. B* **69**, 241101(R) (2004).
  - [9] M. Lapine, M. Gorkunov, and K. H. Ringhofer, *Phys. Rev. E* **67**, 065601(R) (2003).
  - [10] R. W. Ziolkowski, *Phys. Rev. E* **63**, 046604 (2001); R. W. Ziolkowski and A. D. Kipple, *ibid.* **68**, 026615 (2003).
  - [11] V. M. Agranovich, Y. R. Shen, R. H. Baughman, and A. A. Zakhidov, *Phys. Rev. B* **69**, 165112 (2004).
  - [12] G. D'Aguanno, N. Mattiucci, M. Scalora, and M. J. Bloemer, *Phys. Rev. Lett.* **93**, 213902 (2004).
  - [13] W. T. Lu, J. B. Sokoloff, and S. Sridhar, *Phys. Rev. E* **69**, 026604 (2004).
  - [14] X. Huang and W. L. Schaich, *Am. J. Phys.* **72**, 1232 (2004).
  - [15] J. R. Thomas and A. Ishimaru, *IEEE Trans. Antennas Propag.* **53**, 1591 (2005).
  - [16] G. D'Aguanno, N. Akozbek, N. Mattiucci, M. Scalora, M. J. Bloemer, and A. M. Zheltikov, *Opt. Lett.* **30**, 1998 (2005).
  - [17] N. Lazarides and G. P. Tsironis, *Phys. Rev. E* **71**, 036614 (2005).
  - [18] I. Kourakis and P. K. Shukla, *Phys. Rev. E* **72**, 016626 (2005).
  - [19] M. Scalora, M. S. Syrchin, N. Akozbek, E. Y. Poliakov, G. D'Aguanno, N. Mattiucci, M. J. Bloemer, and A. M. Zheltikov, *Phys. Rev. Lett.* **95**, 013902 (2005).
  - [20] G. P. Agrawal, *Nonlinear Fiber Optics*, 3rd edn. (Academic, San Diego, 2001).
  - [21] M. J. Potosek, *Opt. Lett.* **12**, 921 (1987).
  - [22] N. C. Kothari and S. C. Abbi, *Prog. Theor. Phys.* **83**, 414 (1990).
  - [23] R. A. Fuerst, D.-M. Baboiu, B. Lawrence, W. E. Torruellas, G. I. Stegeman, S. Trillo, and S. Wabnitz, *Phys. Rev. Lett.* **78**, 2756 (1997).
  - [24] L. W. Liou, X. D. Cao, C. J. McKinstrie, and G. P. Agrawal, *Phys. Rev. A* **46**, 4202 (1992).
  - [25] S. C. Wen and D. Y. Fan, *J. Opt. Soc. Am. B* **19**, 1063 (2002).
  - [26] J. B. Pendry, A. J. Holden, W. J. Stewart, and I. Youngs, *Phys. Rev. Lett.* **76**, 4773 (1996).